Author/s:
Hu, G;Guo, Y;Zhao, Q;Xiao, G;Li, KG;May, EF

Title:
Separation of Methane and Nitrogen Using Heavy Reflux Pressure Swing Adsorption: Experiments and Modeling

Date:
2023-05-10

Citation:
Hu, G., Guo, Y., Zhao, Q., Xiao, G., Li, K. G. & May, E. F. (2023). Separation of Methane and Nitrogen Using Heavy Reflux Pressure Swing Adsorption: Experiments and Modeling. Industrial and Engineering Chemistry Research, 62 (18), pp.7114-7126. https://doi.org/10.1021/acs.iecr.3c00094.

Separation of methane and nitrogen using heavy reflux pressure swing adsorption: Experiments and modelling

Guoping Hu[1,2,3,*], Yalou Guo[3], Qinghu Zhao[3], Gongkui Xiao[2], Kevin Gang Li[3,*], Eric F. May[2,*]

[1]Ganjiang Innovation Academy, Chinese Academy of Sciences, Ganzhou, Jiangxi, China, 341119

[2]Fluid Science & Resources Division, Department of Chemical Engineering, the University of Western Australia, Crawley, WA, Australia 6009

[3]Department of Chemical Engineering, the University of Melbourne, Parkville, VIC, Australia 3010

ORCID

Qinghu Zhao: 0000-0002-5714-6989

Yalou Guo: 0000-0003-4052-9681

[*]Corresponding Authors:

Modelling

Prof. Eric May

Email: eric.may@uwa.edu.au

Postal Address: The University of Western Australia,

35 Stirling Highway, Perth, Western Australia, Australia. 6009

Pilot demonstration

Dr. Kevin Gang Li

E-mail: li.g@unimelb.edu.au

Postal Address: Department of Chemical Engineering

The University of Melbourne, Parkville, Victoria, Australia. 3010

All other enquiries

Prof. Guoping Hu

E-mail: gphu@gia.cas.cn

Postal Address: Chinese Academy of Sciences

No. 1 Kexueyuan Rd, Ganxian, Ganzhou, Jiangxi Province, China. 341119

Abstract

Pressure swing adsorption (PSA) is commonly used for the challenging task of separating methane (CH_4) and nitrogen (N_2) gas mixtures. Previously we used pilot-scale tests and process simulations to demonstrate how PSA cycles can be optimized for methane-nitrogen separations by adjusting the feed flow, cycle step time and desorption pressure for a given column size. However, to produce a high-value product stream, dilute feeds with < 25 % CH_4 generally require greater enrichment than can be achieved with optimized conventional cycles. In this work, we investigated the effects of including a heavy product reflux/purge step in PSA cycles on the separation of CH_4/N_2 using ionic liquidic zeolites (ILZ) as adsorbents, through both pilot plant tests and process simulations. In the pilot demonstrations, the use of a heavy purge step allowed the enrichment of feed mixtures with 5.6 % and 25.1% methane to 27.4% and 85.5% with recoveries of 83% and 96%, respectively, which outperforms most reported studies under similar operational conditions. However, while the refluxes increased from 74% to 80%, the recovery of CH_4 dropped from 79% to 75% as CH_4 is lost into the light product stream. Optimum separation performance in terms of CH_4 purity and recovery occurred at a bed capacity ratio for the purge step of $\mathcal{C}_{PU} \cong 0.87$, which could help guide future selections of heavy purge flow rates for a given column size and adsorbent material.

1. Introduction

Methane (CH_4) is a greenhouse gas and the second most significant driver of anthropogenic climate change[1, 2]. The CH_4 level in the atmosphere has reportedly increased from 1700 to 1924 parts per billion in approximately 30 years[3, 4], in part due to emissions from industrial processes such as the production, transport and use of natural gas and coal seam gas[5-7]. Capturing CH_4 from mixtures that would otherwise be vented to the atmosphere is seen as one of the most important and cost-effective opportunities to significantly reduce greenhouse gas emissions in the near future.

The upgrading of methane from biogases often consists of two steps, a CO_2 removal process followed by N_2 rejection. The nitrogen contents are often between 0 and 33%. Coal seam gas may contain 0.5 to 99% CH_4 with N_2 or air as balance gases, and approximately two thirds of coal mines emitting gas contains a CH_4 concentration below 25%[8]. The separation of CH_4 from mixtures with nitrogen (N_2) is, however, a significant challenge given the similarity in their molecular and thermodynamic properties[9]. Various technologies have been investigated and used to separate CH_4 and N_2, such as pressure swing adsorption (PSA), membranes, cryogenic distillation, and solvent absorption[10-15] in the laboratory and at industrial scale. PSA cycles are commonly used for a wide range of flow rates and feed concentrations due to their flexibility, high separation efficiency and operational robustness[16].

PSA is commonly used for many gas separations, such as carbon dioxide capture, hydrogen purification, air separation and natural gas processing[17-22]. A wide range of advanced PSA cycles have been developed to achieve higher product purity, recovery, productivity, and/or energy efficiency for the particular separation process. A range of novel PSA processes has been proposed and demonstrated particularly for the purpose of upgrading dilute mixtures of CH_4 in N_2 or air. May et al. investigated the separation of CH_4 and N_2 using dual-reflux PSA with activated carbon, Engelhard titanosilicate type 4 (ETS-4), and ionic liquidic zeolites as adsorbents, via experiments and simulation[23-25]. Results showed that optimised DR-PSA processes using Norit RB3 adsorbents can upgrade dilute methane (2.4 %) to 35.7 %, leaving a clean nitrogen vent bearing 3000 ppmv methane, which is promising in the reduction

of fugitive methane emissions. Guo et al. employed a triple-reflux strategy to separation CH_4/N_2/He by opening a third channel on DR-PSA[26] and achieved three high purity streams simultaneously. Rodrigues and Li et al. used a more adsorptive component (CO_2) to displace the adsorbed CH_4 and achieved 75% CH_4 product with 89% recovery from 10% CH_4 [27, 28]. Recently, Li et al. employed a pure methane displacement strategy to achieve 99% CH_4 from 10% CH_4 using simulated moving beds[29].

Two primary methods are usually explored in efforts to improve the performance of CH_4/N_2 separations using PSA processes. One method is to develop better adsorbent materials that have increased selectivity for either CH_4 or N_2. A range of commercially available adsorbents have been widely deployed to separate CH_4 from N_2 such as activated carbon, ETS-4, carbon molecular sieves and zeolites [30-35]. Recently, Li et. al.[2, 36] developed a new adsorbent named Ionic Liquidic zeolite (ILZ), which has shown better separation performance than activated carbon and ETS-4 in separating CH_4 and N_2 under similar operating conditions[33, 37-39]. In our previous publication, we demonstrated through a combination of pilot-scale tests and process simulation how conventional PSA cycles using ILZ could be optimised to enrich dilute methane-in-nitrogen mixtures from CH_4 concentrations of 5 – 16% to 12 – 45% [8]. However, more concentrated CH_4 product is needed for utilization, either for power generation or household purposes. Hence, the development and demonstration of PSA cycles with an increased capacity for enrichment is necessary.

Dual-reflux and triple reflux PSA cycles, demonstrated at laboratory-scale and via numerical simulations utilise continuous heavy reflux flows, and have been shown to achieve substantial enrichments of dilute methane-in-nitrogen mixtures[25, 33, 37-39]. However, these more complex PSA processes have high capital and operational costs, which could limit their large-scale application. Heavy reflux, also known as heavy product displacement or heavy purge, is one cycle modification that introduces a sub-stream from the heavy product to purge the adsorption column after adsorption steps. As the heavy stream has higher adsorbate concentration than the feed gas, the heavy purge can partially replace the less adsorptive gas due to competitive adsorption on adsorbents and purge the free gas (often less adsorbed gas) out of the column. Therefore, heavy reflux is often used to increase

the enrichment of adsorbate achieved by PSA processes[40, 41]. Reynolds et al.[42, 43] compared a few heavy reflux configurations for CO_2 capture from flue gases with a combination with light reflux and a recovery or feed plus recycle step. Those results showed a clear trade-off relationship between CO_2 recovery and purity. However, the effect of heavy purge in methane enrichment is not well investigated.

In this work, a heavy purge step, which allows a heavy product sub-stream to be injected to the adsorption column, is introduced to the conventional PSA process, aiming at a higher heavy CH_4 concentration by reducing the dilution effect of the residual gases in the void space and obtain higher CH_4 uptake via competitive adsorption against N_2. The impact of the heavy product purge step is investigated using a combination of pilot scale experiments and process simulations. Adding a heavy purge step to a conventional PSA cycle does not excessively increase the complexity of the process, and has been practiced to improve the purity of the heavy product stream[42]. The goals of this work are (1) to demonstrate its capacity to adequately enrich dilute CH_4 in N_2 feeds as often generated by coal mine vents, and (2) to develop a quantitative framework for deciding the level of heavy purge that should be applied to achieve an optimal separation performance.

2. Methods

2.1 Pilot plant tests

The pilot experiments were conducted using a 6-column PVSA facility, the details of which been mostly described in our previous work, so only a brief summary is given here [8, 44]. Six identical columns with a diameter and height of 0.15 and 2.00 m, respectively, were packed with three layers of adsorbents sourced from Gas Capture Technologies Pty, Ltd., Australia[45], namely alumina (AL, 2.6±0.1 kg), activated carbon (AC, 2.7±0.1 kg) and ionic liquidic zeolites (ILZ, 18.7±0.2 kg) from bottom to top. The ILZ adsorbents, cation exchanged using ionic liquids on FAU zeolites, were reported with a high CH_4/N_2 selectivity (6–8 at equimolar concentrations)[36]. Both the ILZ and alumina were white or light-yellow spherical beads, while the activated carbon consisted of black flakes. The alumina and activated

carbon were selected as guard layers to remove trace amount of water and heavy hydrocarbons, respectively, to maintain the ILZ's high selectivity for CH_4 over N_2. All adsorbents were activated at 180 ^oC for 3 hours using a hot N_2 stream prior packing. The isotherms and physical properties of the adsorbents were reported in our previous work and are provided in the Supporting Information (Table S1 and Figure 1)[8, 30].

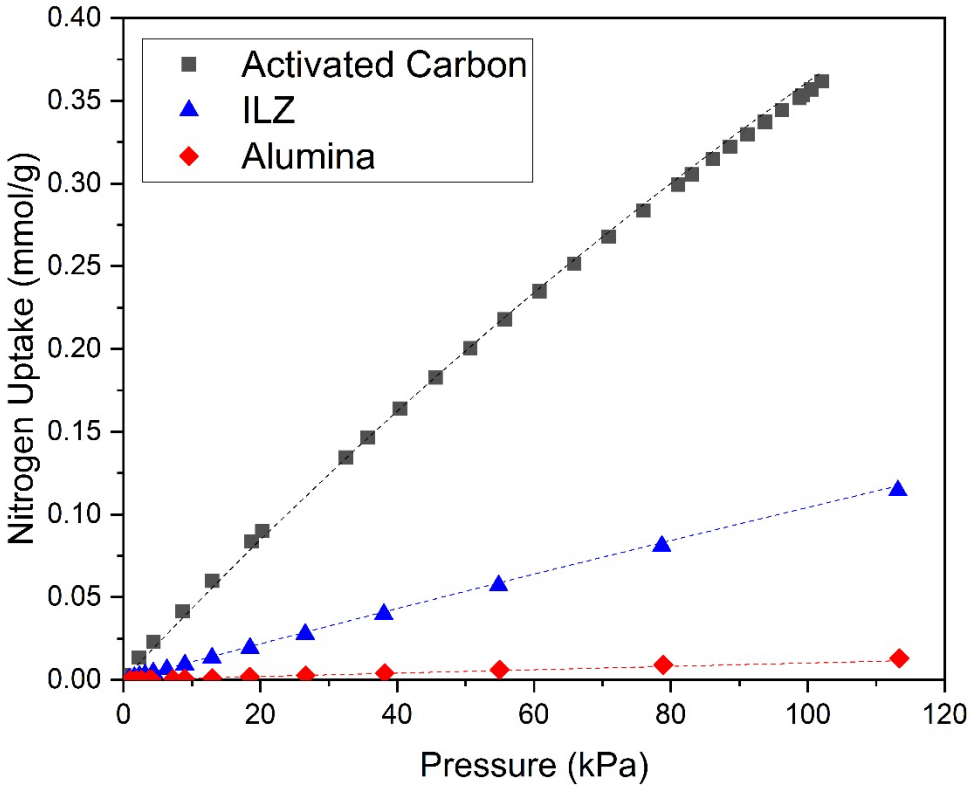

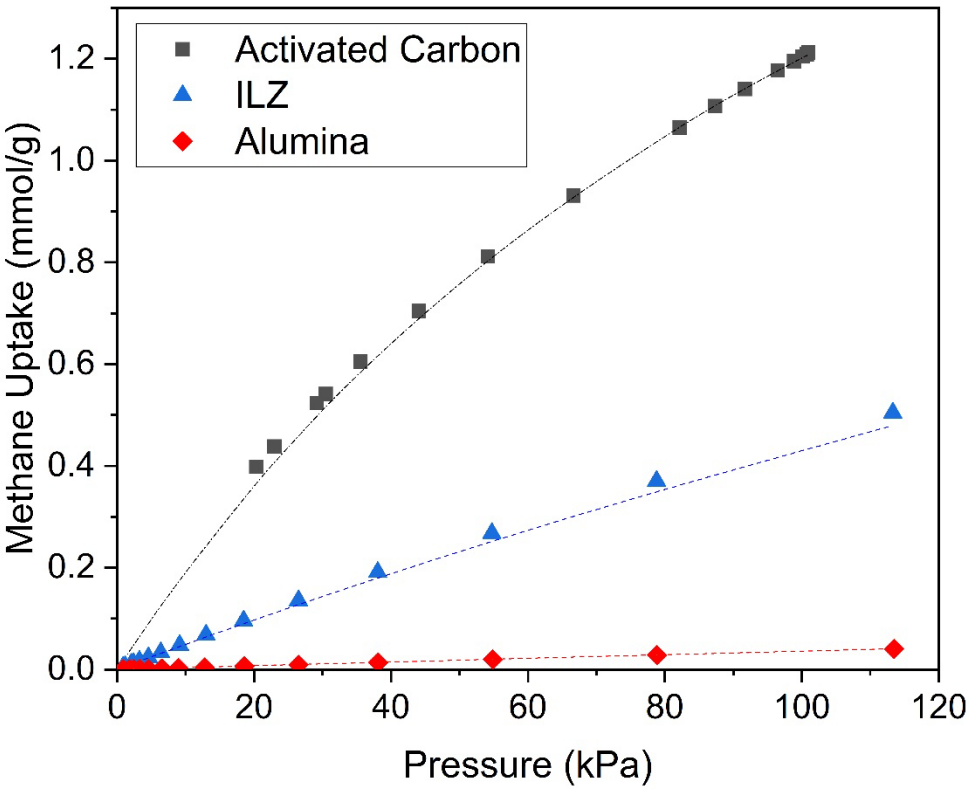

Figure 1. The measured adsorption isotherms and fitted results using Langmuir model of CH_4 and N_2 on the alumina (303 K), activated carbon (294 K), and ILZ (303 K) (Dots denote the measured isotherms and line represents the fitted results using Langmuir model).

The feed gases were mixed using town gas and pure N_2 at room temperature. Impurities such as water vapour and heavy hydrocarbons were below 0.5 mol.% and not monitored during the pilot plant tests. The flowrates of feed, heavy and light gas streams was measured using G16 Diaphragm gas flow meters (0.16–25 m^3/h, Chongqing Shancheng Gas Equipment Co., Ltd.). A dry scroll vacuum pump (DPB020, 0.75 KW, Shanghai AfaPa Vacuum Equipment Co., ltd) was used for the regeneration of adsorbents. The energy consumption was estimated by assuming full load of the pump. The pressure was monitored using differential pressure sensors (-0.1–1.0 MPa, Changhui Analytical Instrument Co., Ltd.). The concentrations of CH_4 were measured using and QGS-084 infrared analysers (0–100%, Beijing BAIF-Maihak Analytical Instrument Co., Ltd.). Unfortunately, the test facility had no capacity to

reliably measure the heavy purge flow rate, so the pilot tests could only demonstrate its effectiveness at increasing product purity in tandem with the modelling study described below. The operating pressure was recorded via transducers located at the top of each column. The recovery (R) of CH_4 was calculated using *Equation 1*, where F_H and F_{fed} were the flowrates of heavy product and feed gas, respectively, and c_H and c_{fed} were the CH_4 fractions in the heavy product and feed gas, respectively. The productivity (Y) of CH_4 was calculated by *Equation 2*, where m was the mass of adsorbents.

$$R = \frac{F_H \cdot c_H}{F_{fed} \cdot c_{fed}} \times 100\% \qquad \textit{Equation 1}$$

$$Y = \frac{F_{fed} \cdot c_{fed} \cdot R}{m} \qquad \textit{Equation 2}$$

The design of PSA cycles is highly dependent on the properties of the required product and adsorbents, which can include a range of operations such adsorption, pressure equalization, desorption, idle and product purge. The PSA cycle (Figure 2) used in this work was a simple modification of the cycle reported previously[8]. In this work, the six-bed system is required to treat feed gas and produce products continuously. Therefore, there is always one bed under adsorption and the other under desorption simultaneously. Each of the six columns undergoes the same steps in a full cycle, however, with a time delay of 1/6 cycle, respectively. Additional pressure equalization steps are added to increase the recovery of methane and decrease the energy penalty. A repressurization/light purge step is also considered as measures to increase methane recovery and avoid the fluidization of adsorbents resulted from high gas flowrates. The number of idle steps is required to be as less as possible to improve the cycle efficiency. An extra heavy purge step (Step 5) was added to introduce a sub-stream from the product stream evacuated from the columns. Each cycle consisted of 18 steps: i.e., adsorption (Steps 1−3), pressure equalization (PE, Step 4, 6, 7, 15−17), heavy product purge (HP, Step 5), desorption (Step 10−12), light product purge (or repressurization, Rep or LPU, Step 18) and idle steps (Step 8, 9, 14). The idle steps were inserted to permit scheduling. The cycle duration was controlled by step time. The total cycle time of 1080 s was required to allow the vacuum pump

sufficient time (180 s) to evacuate each column effectively in all pilot tests and simulations[8]. The step times were set at 60 s.

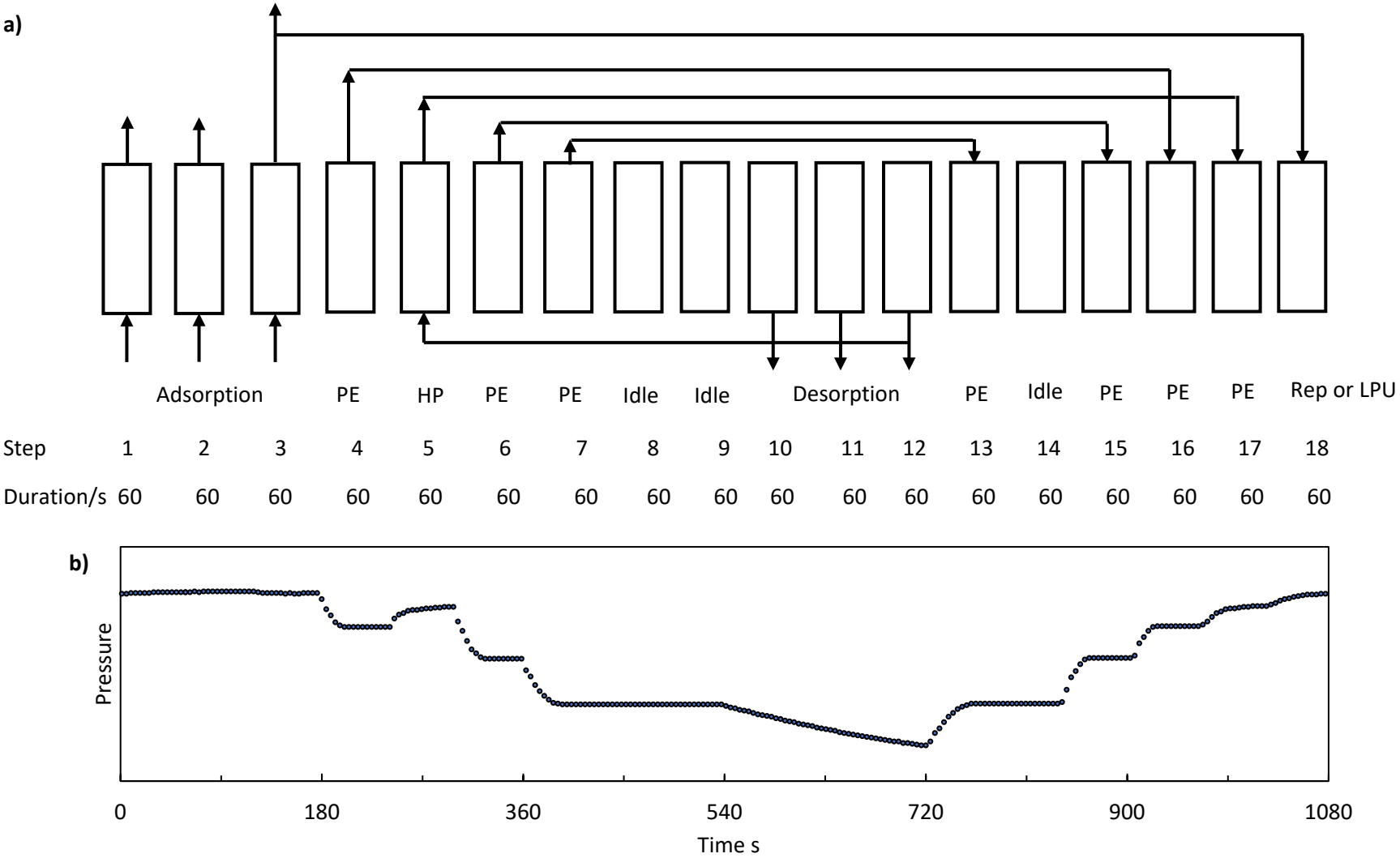

Figure 2. a) Schematics and cycle sequences of the 6-column heavy reflux PSA cycle; b) the measured pressure variations in a typical PSA cycle, with the duration of each cycle set as 1080 s.

2.2 Simulation

The numerical model was built on the Aspen Adsorption platform, which was validated and used in our previous work[8, 44]. Momentum balance was calculated using the Ergun Equation and axial dispersion was neglected. The binary adsorption isotherms and kinetics were calculated using the extended Langmuir model and lumped (linear) resistance model, respectively. The Implicit Euler method was used as the integration method. The cyclic operation of this model was controlled using a cycle organizer. Gaussian elimination MA48 and mixed Newton method were used as the linear and nonlinear solvers, respectively. The detailed assumptions and governing equations used are given in the Appendix I (S1.0).

Figure S1 shows a screenshot of the model used to simulate the cycle presented in Figure 2. Relative to the simulation detailed previously, a variable heavy purge flow, VHPU, was taken from the heavy product tank (B08) using control valve HPU. This heavy purge flow was routed to the bottom of each column, where it could be admitted at relevant stage in the cycle using valves A06−F06. The heavy purge ratio (*HPR*, *Equation 3*) was defined as the fraction of the gas flowrate purged to the column (F_{HP}) and the gas flowrate evacuated from the column (F_{Ev}).

$$HPR = \frac{F_{HP}}{F_{Ev}} \qquad \textit{Equation 3}$$

2.3 Process and energy analysis

As the adsorption pressure in the studied system was only slightly above the atmospheric pressure (1.2 bar), and feed gases were often used as provided in practice, the compression energy consumption was ignored and only evacuation work (*W*) was considered in the energy analysis. The energy consumption of the vacuum pump per mole of CH_4 produced was calculated using *Equation 4*[24], where *γ* was the ratio of specific heats, *R* was the gas constant, *T* was the temperature, P_{Dis} was the discharge pressure of the pump (1 bar), P_{Vac} was the average vacuum pressure, *η* was the pump efficiency and set to be 0.7[27, 30, 46, 47].

$$W = \frac{\gamma RT}{\eta(\gamma-1)}\left(\frac{P_{Dis}}{P_{Vac}}^{\frac{\gamma-1}{\gamma}} - 1\right) \qquad \textit{Equation 4}$$

2.4 Bed working capacity

The bed capacity ratio $\mathbb{C}$ is a dimensionless quantity introduced by Bhatt et al.[48] and adapted by May and co-workers[25, 38] to help quantify utilisation of the bed, independent of the particular column dimensions and feed flow rate in DR-PSA cycles. Recently, we further expanded the concept to conventional PSA cycles[8]. For PVSA cycles that include heavy purge steps it is necessary to define a bed capacity ratio for each step during which gas with appreciable concentrations of the adsorbate (methane) flow into the bed. In this work it was necessary to define a bed capacity ratio for both the feed step, $\mathbb{C}_{FE}$, and for the heavy purge step and $\mathbb{C}_{PU}$. The former was defined in this work as follows:

$$\mathbb{C}_{FE} = \frac{F \cdot y_F \cdot t_{FE}}{n_A^{gas} + n_A^{ads}} \qquad \textit{Equation 5}$$

$$n_A^{gas} = y_H \times \frac{p_H V_{bed} \varepsilon}{RT} \qquad \textit{Equation 6}$$

$$n_A^{ads} = \sum_i [m_{ads,i} Q_{i,A}(p_H, T, y_H) - m_{ads,i} Q_{i,A}(p_L, T', y'_H)] \qquad \textit{Equation 7}$$

Here F is the feed gas flowrate, y_F is the methane fraction in the feed gas, t_{FE} is the feed step time, p_H and T are, respectively, the (high) pressure and temperature of the adsorption step, V_{bed} is the volume of the bed, ε is bed's the void fraction, and $m_{ads,i}$ is the mass of adsorbent type 'i' in the bed (when multiple layers of adsorbent are used). The maximum amount of methane that can be stored in the gas phase (void space) is quantified by n_A^{gas}, calculated using *Equation 6* with y_H being the methane fraction in the heavy product. The working capacity of the adsorbent, n_A^{ads}, calculated using *Equation 7* represents the maximum change in the quantity of adsorbate that the packed bed can treat given the cycle conditions: $Q_{i,A}(p_H, T, y_H)$ is the equilibrium capacity of adsorbent 'i' evaluated at the heavy product's concentration, while $Q_{i,A}(p_L, T', y'_H)$ is the capacity evaluate under the desorption step's pressure, p_L, temperature T' and methane concentration, y'_H.

The bed capacity ratio for the purge step (Step 5, Figure 1), $\mathbb{C}_{PU}$, is defined similarly using *Equation 8* to characterize the extent to which the bed is being used, with $n_{A,PU}$ denoting the amount of methane in the purged gas flow. The quantities F_{PU}, y_{PU} and t_{PU} in *Equation 9* are the flowrate, CH_4 concentration and duration of the purge step, respectively.

$$\mathbb{C}_{PU} = \frac{n_{A,PU}}{n_A^{gas} + n_A^{ads}} \qquad \textit{Equation 8}$$

$$n_{i,Purge} = F_{pu} \cdot y_{pu} \cdot t_{pu} \qquad \textit{Equation 9}$$

Hu et al.[8] showed how the bed capacity ratio of the feed step provided a useful variable for correlating cycle and bed parameters against a single metric for separation performance, Θ, defined as the product of CH_4 purity and recovery.

$$\Theta = y_H \times R \qquad \textit{Equation 10}$$

In this work, the simulated feed step parameters were held constant near the optimum identified, and only the purge step parameters were varied. Thus, the correlation between $\mathbb{C}_{PU}$ and Θ was explored through the simulations, primarily by adjusting F_{PU} to identify the value of $\mathbb{C}_{PU}$ at which Θ reached a maximum.

3. Results and discussion

3.1 Pilot demonstration test results

Table 1 shows the pilot test results using different feed gas concentrations, i.e., 6%, 16% and 25% CH_4 in N_2. The feed gas pressures were 121±3 kPa, while the desorption pressures were between 20 and 29 kPa. All pressure data are absolute values unless otherwise specified. The environment temperature was between 8 and 12 ^oC for all of the tests. Cyclic steady state was usually achieved within 20 cycles (approximately 5 hours) as determined by the concentrations of both the light and heavy products being stable (±0.2%). A further 2 hours operation was then used for data acquisition. In each trial (No. 1−6), the CH_4 concentration in the light product stream was below 1.5%. The recovery

of CH_4 was higher than 80%. Trial 7 and 8 are from our previous work[8] using a PSA cycle without heavy purge.

The operational pressure profiles have been provided in Figure 2. Results show a clear correspondence of the pressure variation with time. The second adsorption step at time 120 s shows the highest pressure and the lowest pressure value occurs at the end of desorption step at time 720 s. The corresponding temperatures are shown in Figure S2 in Appendix 1. As the temperature sensor is installed inside a thermowell, there is a clear delay between the pressure and temperature profiles. Simulations were also conducted to verify the model by anchoring the flowrate of the heavy product streams with the pilot results. The comparison of methane product concentrations between pilot demonstration and simulation are shown in Figure 3. The corresponding pressure profile are shown in Figure S3. The simulated results agree with the pilot results. However, the temperature profiles (Figure S4) from the pilot demonstration also have a short period of delay, which is likely due to the measurement delay from the thermowell.

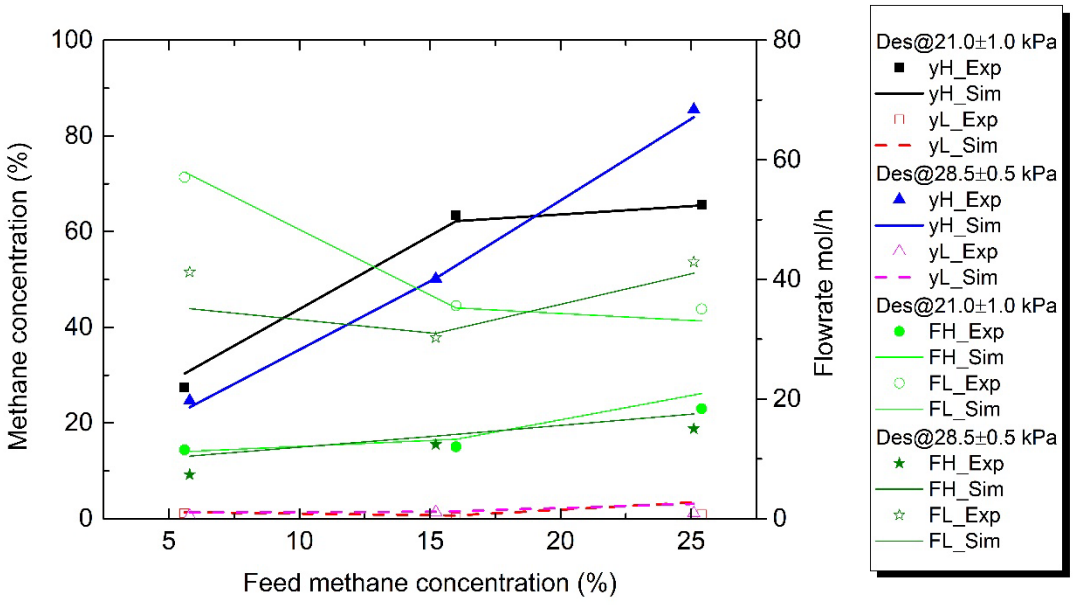

Figure 3 A comparison between experimental and simulated methane product concentration with the change of feed methane concentrations.

Table 1 A comparison of pilot trials results from this work, including two measurements reported previously with the same facility but no heavy purge step.

Trial No.	Environment temperature °C	Adsorbents	Pressure, kPa.a		Concentration, CH_4%			Feed flow, mol/h	Recovery, CH_4%	Productivity, CH_4 mol/kg/h	Estimated Energy J/mol CH_4	Source
			Adsorption	Desorption	Feed	Product	Exhaust					
1	12	ILZ	118	20	5.6	27.4	1.2	68.8	83	0.022	276	This work
2	12	ILZ	123	28	5.8	24.6	0.6	45.3	85	0.016	381	This work
3	10	ILZ	118	20	16.0	63.4	0.3	47.9	98	0.052	116	This work
4	8	ILZ	120	28	15.4	50.2	1.4	42.9	93	0.042	143	This work
5	10	ILZ	122	22	25.1	85.5	1.2	57.5	96	0.094	64	This work
6	11	ILZ	123	29	25.4	65.6	0.9	53.0	98	0.090	67	This work
7	17	ILZ	118	23	5.0	11.5	1.4	47.0	82	0.013	-	[8]
8	19	ILZ	122	21	16.1	34.6	3.1	85.8	89	0.084	-	[8]

3.1.1 Effects of feed gas concentration

As shown in Table 1 and Figure 4, CH_4 purities in the heavy product stream increase proportionally with feed CH_4 concentration, while maintaining the light product's CH_4 concentration below 1.5%. The methane enrichment ratio is between 2.6 and 4.9, which is higher than those reported in literature for similar PVSA cycles without a heavy purge step.[8, 49]. Feed gas with 5.6% CH_4 was upgraded to 27.4% with a recovery of 83% using a desorption pressure of 20 kPa. The heavy product CH_4 purities of 63.4% and 50.2% were produced from a feed of 15.7±0.3 % CH_4 with recoveries of 98% and 93%, using desorption pressures of 20 and 28 kPa, respectively. Such product gases can be used as fuel gases for power generation or low-grade town gases[50-52]. Heavy product CH_4 concentrations higher than 85% were produced by upgrading feed gases with CH_4 concentrations over 25% with a high recovery of 96% using an evacuation pressure of 22 kPa, sufficient to meet pipeline gas specifications[50].

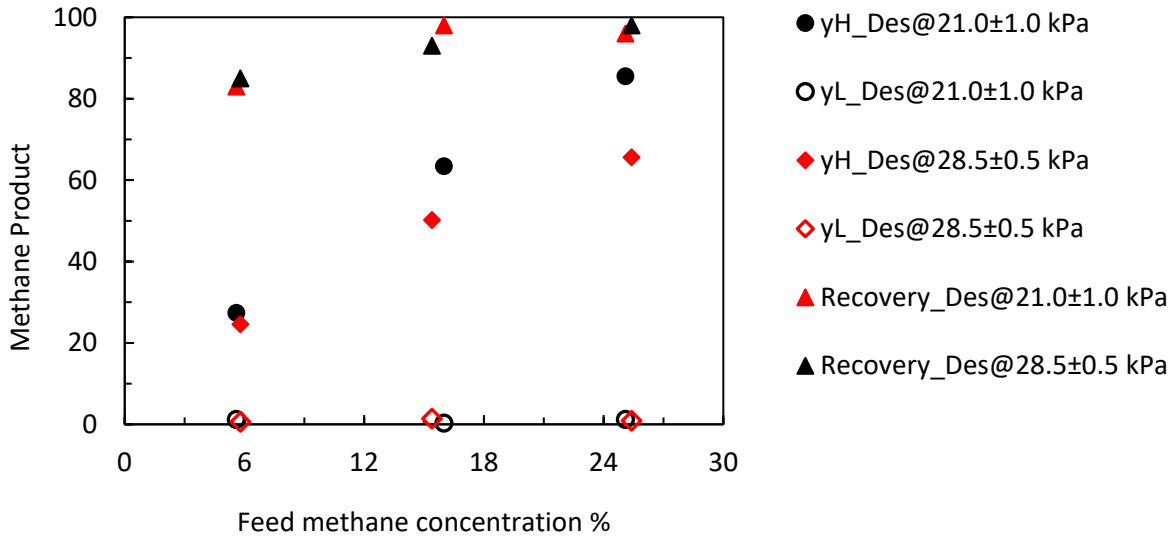

Figure 4. Methane product concentrations and recoveries in the heavy, y_H, and light, y_L, product streams from the pilot tests for various feed concentrations ranging from 6 to 25% and desorption pressures of 21.0 to 28.5 kPa.

3.1.2 Effects of desorption pressure

Figure 5 shows a comparison of the methane product purities resulting from two desorption pressures at three feed gas concentrations. The methane recoveries measured at the same feed concentration

were similar (Table 1), i.e., 84±1% for 5.7% feed, 96±3% for 15.7% feed and 97±1% for 25.2% feed. Results show that lower desorption pressures largely increased the product purity: a reduction from 28.5 to 21.0 kPa increased the product purity by 12%, 26% and 30% for feed gas of 5.7%, 15.7% and 25.2%, respectively. These results are mainly attributed to the increased working capacity of the adsorbents while decreasing the desorption pressures.

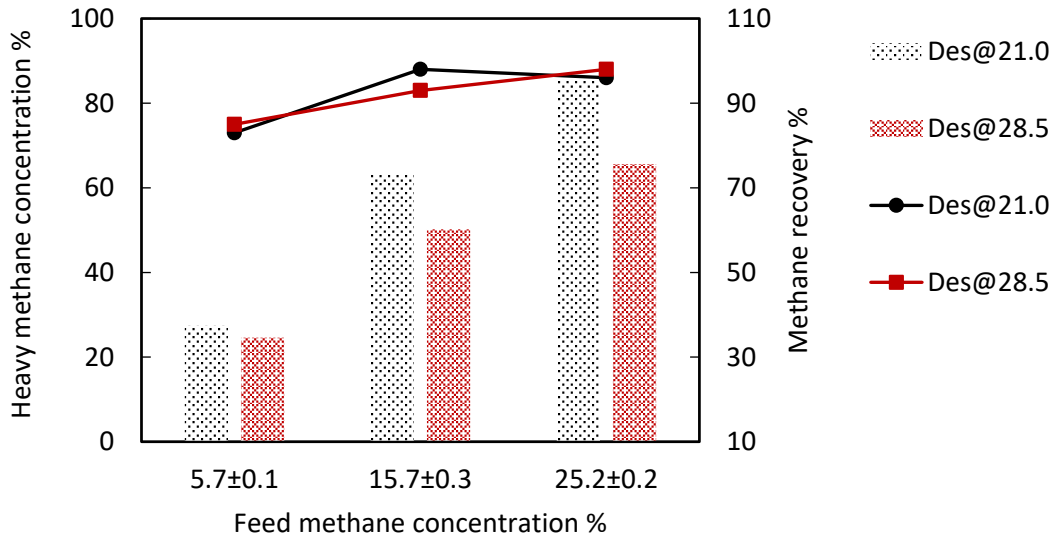

Figure 5. Comparison of methane product purity at different desorption pressures (dots denote the recovery of methane and bars are the methane concentration in the heavy streams).

3.1.3 Effects of heavy product purge

Figure 6 shows a comparison of the heavy product CH_4 purities achieved in the pilot demonstrations from similar feed concentrations and vacuums using cycles with and without a heavy purge step. Although heavy purge steps have been widely reported to increase the heavy product purity in various operations, mostly applied in carbon capture processes, the reported heavy component recoveries are often quite low 30−70%[53-55]. The PVSA cycle with heavy purge steps demonstrated in this work using the pilot plant achieved four times enrichment of the CH_4 purity with high recoveries in the range 83 to 98 %. For the feed gases with methane concentrations of 5.6% and 16.0%, introducing a heavy purge step approximately doubled the enrichment achieved in both cases while the recoveries were

similar or improved. The detailed impacts of heavy product purge will be discussed in detail in Section 3.2.

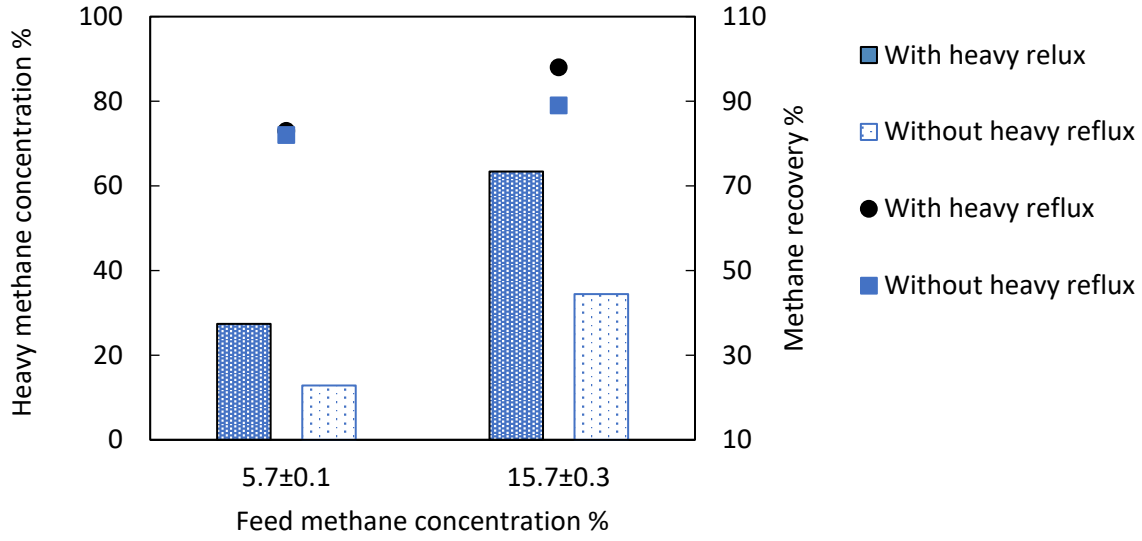

Figure 6. Effects of adding a heavy purge step to the methane product concentration (dots denote the recovery of methane and bars are the methane concentration in the heavy streams).

3.1.4 Comparison with literature results

Figure 7 shows a comparison of methane upgrading results with literature using PVSA cycles. The detailed data can be accessed in Appendix II. The adsorption pressure is below 700 kPa and regeneration is achieved under evacuation pressures below 31 kPa. The operational temperatures are in between 10 and 25 ^{o}C, which are local ambient conditions. The simulated moving bed with a displacement stream using pure methane or carbon dioxide[29, 56] shows superior performance over conventional PVSA cycles. However, among conventional PVSA cycles, methane enrichment results from this study outperforms most of the literature reports under similar recoveries and operational conditions.

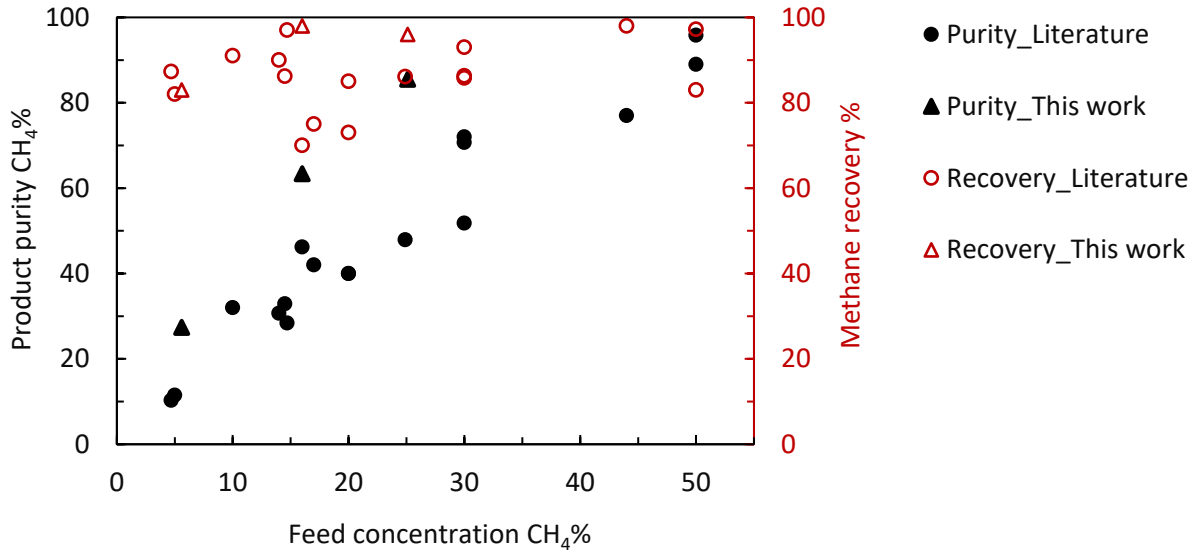

Figure 7 A comparison of methane upgrading performance in this work with literature reported results[8, 30, 44, 46, 49, 57-59]. The operations are mostly under ambient temperatures, adsorption within the range of 1 to 20 bars and desorption at 7 to 140 kPa. Original data is available in Appendix II.

3.2 Simulation

To better understand how introducing the heavy purge step resulted in the significantly improved separation performance observed (Section 3.1) in pilot tests, simulations of the PVSA process and used to more systematically investigate the impact of the purge flow on the CH_4/N_2 separation and overcome limitations of the experimental pilot facility. The effects of the heavy purge flow were studied under otherwise fixed operational conditions, i.e., feed CH_4 concentration of 15%, feed flowrate of 60 mol/h, adsorption pressure of 120 kPa, desorption pressure of 21.5 kPa, and an environment temperature of 12 ^{o}C. Numerical results are given in the supporting information (S4.0).

3.2.1 Separation performance

Figure 8 shows the simulated separation performance of the PVSA cycle with heavy purge ratios (Eq 3) ranging from 0 to 0.80. These calculations indicate that increasing the heavy purge ratio monotonically enhances the heavy product purity achieved; however, the CH_4 recovery decreases simultaneously. Compared to a process without heavy purge (HP of 0), the simulation indicates that a heavy purge ratio of 0.74 is needed to produce a heavy product purity of 61%, which is consistent with

the results obtained for Trial 3 of the pilot demonstrations, which had a similar feed concentration and desorption pressure. Increasing the heavy purge ratio further from 0.74 to 0.80 enhances the product concentration by another 10%, but causes the recovery of CH_4 to drop from 79% to 75%.

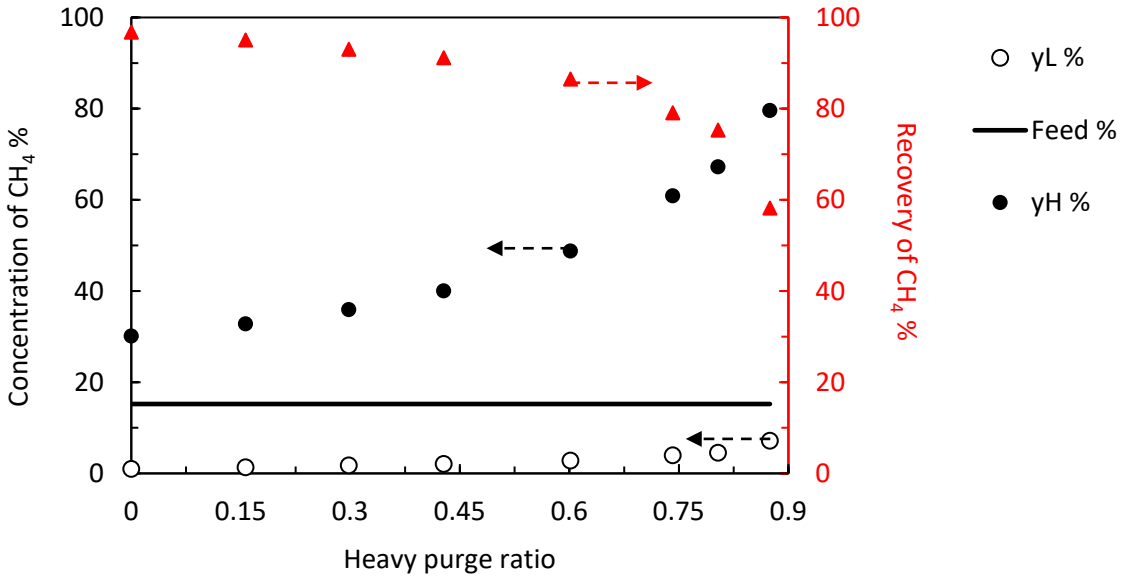

Figure 8. Effect of heavy purge ratio on the heavy product CH_4 purity and CH_4 recovery.

3.2.2 Cyclic profiles

The gas phase CH_4 concentrations at the top, middle and bottom of the adsorption column A are shown in Figure 9 together with the corresponding pressure profile for a heavy purge ratio of 0.60 as an example. During adsorption (Steps 1−3, 0−160 s, Figure 1), the CH_4 concentration at the bottom (0) of the column (1) decreases rapidly to the feed gas concentration (15.2%) and stabilizes. The column pressure is then equalized with another column (Step 4, Figure 1) from 160 to 180 s. During this step, the column pressure drops from 120 kPa to 101 kPa and the CH_4 concentration at the bottom of the column slightly increases due to desorption. Thereafter, the heavy purge stream, which is drawn from the heavy product buffer tank, is injected to the column (Step 5, 180−200 s, Figure 2). A surge in CH_4 concentration can be seen at the bottom of the column, from 16% to 49%, reaching the concentration of the heavy product, while the composition of the gas located in the upper part of the column is only half of that at the bottom. The column then undergoes two pressure equalization steps (200−480 s).

During the desorption (Steps 10−12, 160−480 s, Figure 1), the CH_4 concentration in the column bottom first increases from 52% (480 s) to 60% (488 s), then decreases to 42% (558 s), before returning to 44% (640 s).

The maximum CH_4 concentration in the column occurs at 488 s. This is mainly due to two reasons. First the feed and heavy purged gas are injected from the bottom of the column and therefore adsorbents in this region uptake more CH_4 than they do in the upper part of the column (Figure 9) [46, 47, 57]. Second, the pressure equalization steps drop the column pressure from 110 kPa to 50 kPa, causing CH_4 to desorb into the gas phase. Both contribute to the CH_4 concentration spike in the first a few seconds following the start of the desorption pressure step. As evacuation continues, desorption continues, as indicated by the CH_4 concentration incline, leading to the second peak at 640 s.

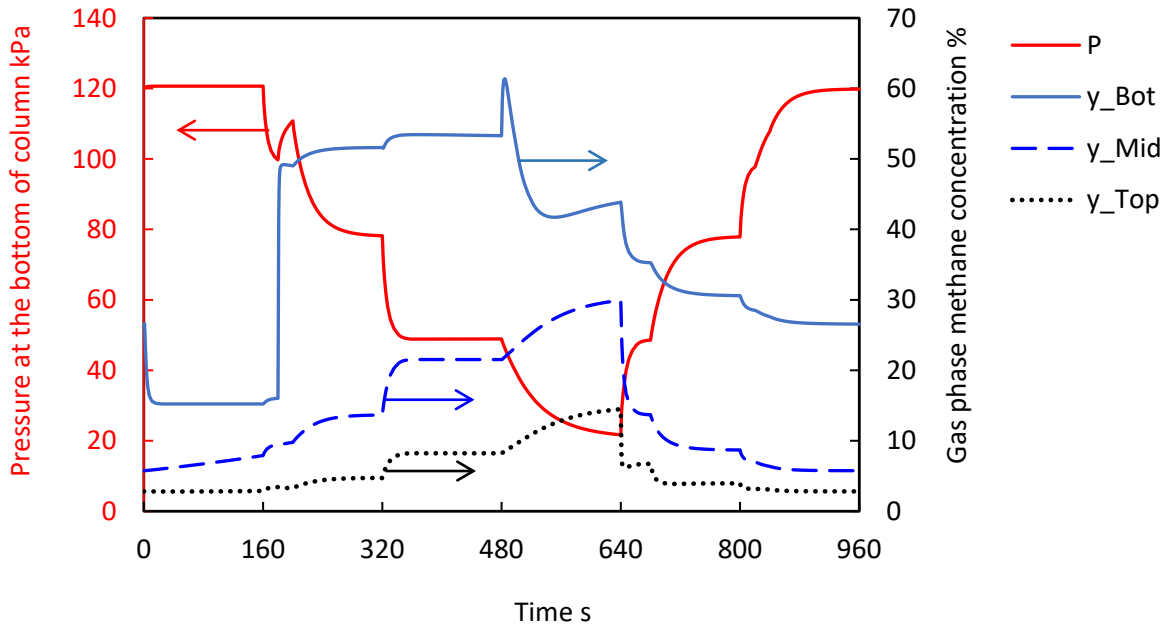

Figure 9. The CH_4 concentrations in the gas phase at the bottom (fractional column length of 0), middle (fractional column length of 0.5) and top (fractional column length of 1) of the column and corresponding cyclic pressure profile.

3.3.3 Column profiles

As shown in Figure 10, four time slots are selected as key indicators of the process operation, which are at the end of adsorption (160 s), start of purge (180 s), end of purge (200 s) and end of desorption (640 s). The maximum gas uptake by the bed occurs at the end of the adsorption. The difference in gas loadings between the start and end of the purge step reflects the majority of the purged gas returned to the bed. End of desorption corresponds to the minimum gas loading on the adsorbents. Figure 10 a), b) and c) show cyclic steady state profiles along the bed for the CH_4 concentration in the gas phase, CH_4 loading on adsorbents (solid phase), and N_2 loading on adsorbents at each of these four time slots.

Figure 10a shows that the gas phase CH_4 concentrations in the alumina layer are quite stable, which reflects the low gas adsorption capacity of alumina (see also Figure 10b and c). The CH_4 concentration then drops consecutively in both the activated carbon and ILZ layers. As the CH_4 and N_2 adsorption capacities of activated carbon are higher than ILZ, the loadings of both gases on the activated carbon layer are much higher than those on the ILZ layer. During the heavy purge step, the gas phase CH_4 concentration drops from 49% to 16% sharply in the activated carbon layer, which is due to the high CH_4 adsorption capacity of activated carbon, as shown by the sharp CH_4 loading peak on the activated carbon layer (Figure 10b). Comparing the CH_4 loadings at the adsorption and purge steps, all three layers show increases in CH_4 loading (Figure 10b) and decreases in N_2 loading, which explains why the heavy purge step increases the heavy product CH_4 concentration.

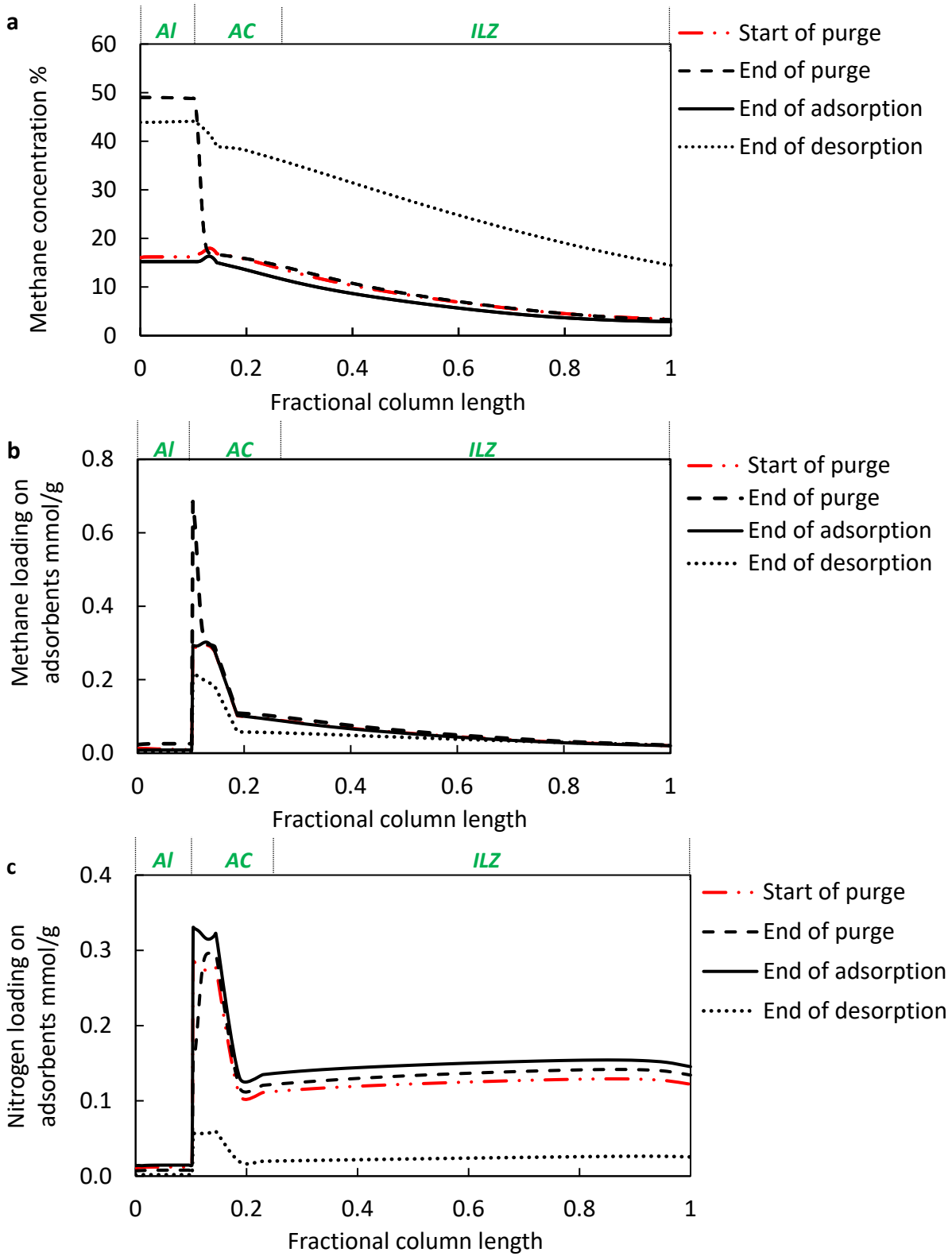

Figure 10. Gas concentration and solid loading profiles along the adsorption column: a) the concentration of CH_4 in gas phase; b) CH_4 loading on adsorbents; c) N_2 loading on adsorbents. The fractional column lengths of 0 and 1 denote the bottom and top of the column, respectively. The labels Al, AC and ILZ denote the alumina, activated carbon, and ILZ adsorbent layers, respectively.

Comparing the gas loadings at the end of adsorption and start of purge in Figure 10b and c, little change is observed for CH_4; however, an obvious drop occurs for the N_2 loading. This phenomenon can be explained as follows. Although the column pressure decreases from 120 to 101 kPa between the end of adsorption and the start of purge, the pressure decrease causes CH_4 desorption and increases the CH_4 concentration in the gas phase (Figure 10a). Thus, the partial pressure of CH_4 is maintained at a stable level and little change in the CH_4 loading on adsorbents occurs. For N_2, however, the partial pressure decreases due to the drop in both the column pressure and the N_2 concentration in the gas phase. Hence, the N_2 loading on the adsorbents drops 0.32 to 0.13 mmol/g from the fractional column length of 0.1 to 0.2. These results also indicate that a co-current depressurization step after the feed step allows the pressure in the column to drop to some specified intermediate pressure, which allows pressure differences for heavy purge and improves the heavy-product enrichment simultaneously[43, 60].

3.3.4 Effects of heavy purge ratio on column profiles

Figure 11 shows the column profiles calculated for different heavy purge ratios ranging from 0 to 0.80 at the end of heavy purge step. The results in Figure 11a show that an 80.4 % heavy purge flow increases the CH_4 concentration in the gas phase from 16% to 67% at the column fraction length of 0. As the heavy purge ratio increases, an increasing concentration CH_4 is re-injected back to the column, causing the adsorption front to move towards the top of the column. The CH_4 concentration at the top of the column increases from 1.3% to 5.5% as heavy purge ratio increases from 0 to 0.80, which leads to more CH_4 being lost to the light product (exhaust) and lower CH_4 recovery for the cycle as shown in Figure 8. In contrast, the N_2 loading on activated carbon shows a contradictory trend to that of CH_4. Taking the column fractional length range of 0.10 to 0.15 as an example, Figure 11c shows how the N_2 loading decreases at higher heavy purge ratios, which reflects the competitive adsorption between CH_4 and N_2.

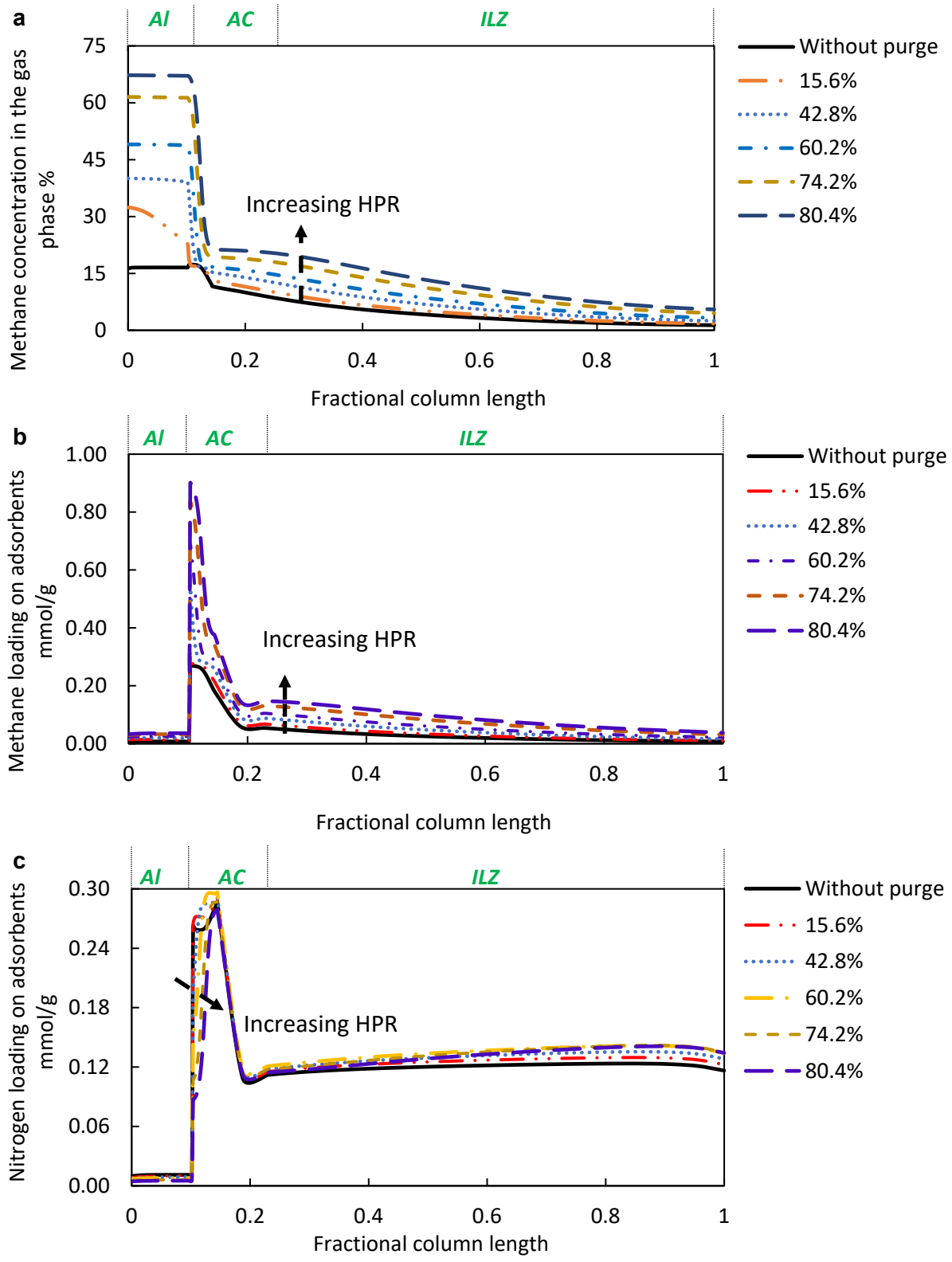

Figure 11. Effects of heavy purge ratio on the column axial profiles: a) concentration of methane in gas phase; b) methane loading on adsorbents; a) the nitrogen loading on adsorbents. The labels Al, AC, and ILZ denote alumina, activated carbon, and ILZ adsorbent layers, respectively.

As shown in Figure 11b, the activated carbon layer seemingly plays a key role adsorbing the CH_4 purged back into the column, given that the CH_4 loading on the activated carbon is much higher than on the ILZ. This is due to two reasons. First, per unit mass, activated carbon adsorbs two times more CH_4 than ILZ under the same pressure, as shown by the adsorption isotherms of the two materials (S3.0). Second, the CH_4 concentration in the gas phase during the heavy purge step is higher at the activated carbon layer than at the ILZ layer. However, as ILZ has a much higher packing density and occupies a large volume than the activated carbon, the cumulative CH_4 adsorbed in the ILZ layer (7.6 mol) is in fact 3 times larger than that in the activated carbon layer (1.9 mol). Hence, the ILZ layer still dominates the CH_4/N_2 separation.

3.3.5 Bed capacity ratio analysis

Figure 12 shows the impact of changing heavy purge ratio on the value of $\mathcal{C}_{PU}$ and the separation performance metric, Θ, at fixed feed flowrate, desorption pressure and step time. $\mathcal{C}_{PU}$ increases with increasing HPR as the purged gas quantity increases proportionally. The optimum separation performance is achieved at a $\mathcal{C}_{PU}$ of 0.87. Further increasing HPR leads to a drop in the separation performance as the reduction in methane recovery exceeds further gains in heavy product CH_4 purity. The loss in recovery reflects a breakthrough of the methane adsorption front into the light product (exhaust) stream, which can be ameliorated by reducing the purge flow or reducing the purge step time. The $\mathcal{C}_{PU}$ optimum of 0.87 is much larger than that found for $\mathcal{C}_{\mathrm{FE}} \approx 0.3$ in our previous work, which reflects the reduced mass transfer zone length generated by a purge flow with a higher CH_4 concentration than the feed gas.

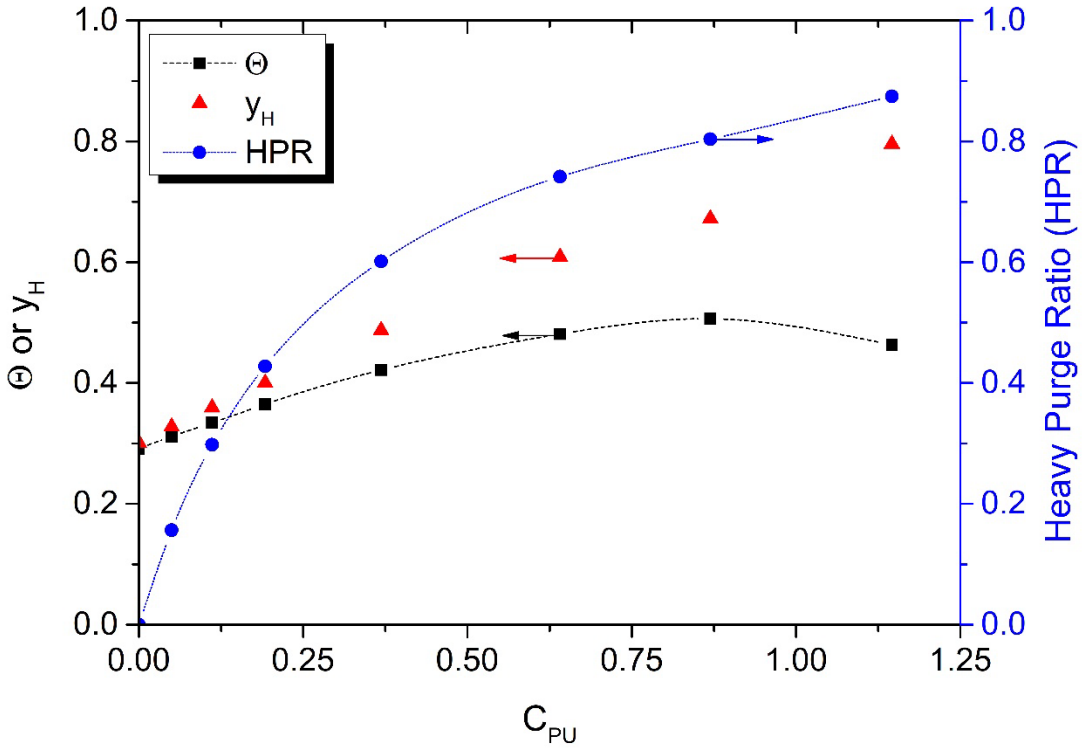

Figure 12. Impact of changing the purge step capacity ratio $\mathbb{C}_{PU}$ defined by Equation 8 on the separation performance, Θ, as defined by Equation 10.

3.3.6 Energy analysis

The calculated energy consumption is between 22 and 185 kJ/mol pure methane at purge ratios of 0 to 0.87, which is at the same order of magnitude with the estimated energy consumption in the pilot demonstration as shown in Table 1 (116 and 143 kJ/mol pure methane for feed gases of approximately 15%). Figure 13 shows how the evacuation energy consumption increases proportionally with product purity and HPR. This is because the heavy product which is purged back to an adsorption column is inevitably evacuated from the vacuum multiple times. Such duplicated evacuation increases the energy required to produce a given amount of heavy product. When the HPR is 74 the enrichment achieved is double that of a cycle without any purge while the energy consumption 1.95 times larger.

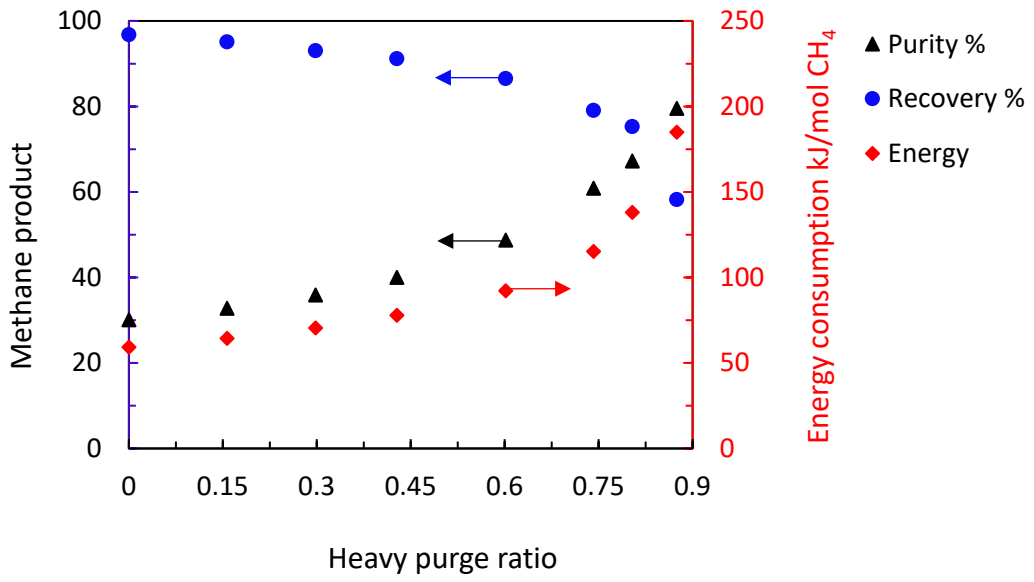

Figure 13. Evacuation work for CH_4/N_2 separation at different heavy purge ratios.

4. Conclusions

The separation of CH_4/N_2 was investigated using a 6-column pressure swing adsorption process packed with three layers of adsorbents (alumina, activated carbon and Ionic Liquidic zeolite (ILZ)) using both pilot plant tests and process simulations. The key focus of this work was to demonstrate and investigate the impact of introducing a heavy purge step on the separation performance. The pilot demonstrations showed that feed gases with 5.6% and 25.1% methane could be enriched to 27.4% and 85.5% with recoveries of 83% and 96%, respectively, making them valuable as fuels for power generation or town gas. The detailed impacts of heavy product purge on CH_4/N_2 separation performance were investigated using process simulations. The product purity achieved from 15% feed gas was 61% while using a 74% heavy purge flow ratio, which is twice the enrichment achieved with a PVSA cycle without heavy product purge. Heavy product purge provides an effective pathway to increase CH_4 uptake and simultaneously decrease N_2 uptake on the adsorbents in the bed. Capacity ratio analysis shows that the maxima in separation performance occurs at the $\mathcal{C}_{PU}$ value of 0.87, a value much larger than the 0.3 found for the feed step. Over purging the system causes separation performance to drop as the recovery decreases with breakthrough of the methane adsorption front

into the exhaust. However, doubling the enrichment achieved using a purge step approximately doubles the cycle duty.

Supporting Information.

Detailed governing equations and parameters used in the simulation supplied as Supporting Information I.

Original data for Figure 7 supplied as Supporting Information II.

Acknowledgements

The authors acknowledge the support from Global Innovation Linkage (GIL) awarded by Department of Industry, Innovation and Science entitled ‘Development of Unconventional Gas Technologies for Sustainable Energy Security’, the discovery project awarded by Australian Research Council entitled Next Generation Gas Separations via Innovative Adsorption Technologies (DP190100983), Early Career Researcher Grants Scheme awarded by the University of Melbourne entitled ‘Production of High Purity Hydrogen from Mixed Pipeline Gases’, Self-deployed Projects of Ganjiang Innovation Academy, Chinese Academy of Sciences and supporting from Jiang Xi Province (Jiangxi Province). Special thanks to technicians at DKT Energy Technology Co. Ltd. for their kind assistance in pressure swing adsorption facilities and plant operation.

Conflict of Interest Disclosure

The authors (EFM, KGL) are also Directors of the company Gas Capture Technologies Pty. Ltd. that supplied the ILZ.

References

(1) Errickson, F. C.; Keller, K.; Collins, W. D.; Srikrishnan, V.; Anthoff, D. Equity is more important for the social cost of methane than climate uncertainty. *Nature* **2021**, *592* (7855), 564-570. DOI: 10.1038/s41586-021-03386-6.

(2) Hu, G.; Li, K. G.; May, E. F. We commercialized a methane capture technology in ten years — here's how. *Nature* **2022**, *604*, 242-245. DOI: 10.1038/d41586-022-00999-3.

(3) Schiermeier, Q. Global methane levels soar to record high. *Nature* **2020**. DOI: 10.1038/d41586-020-02116-8.

(4) Dlugokencky, E.; NOAA/GML. *Trends in atmospheric methane*. 2023. https://esrl.noaa.gov/gmd/ccgg/trends_ch4/ (accessed 2023 1/3).

(5) Heydarzadeh, Z.; Mac Kinnon, M.; Thai, C.; Reed, J.; Brouwer, J. Marginal methane emission estimation from the natural gas system. *Appl. Energy* **2020**, *277*, 115572. DOI: 10.1016/j.apenergy.2020.115572.

(6) Sheng, J.; Song, S.; Zhang, Y.; Prinn, R. G.; Janssens-Maenhout, G. Bottom-up estimates of coal mine methane emissions in China: A gridded inventory, emission factors, and trends. *Environ. Sci. Technol. Let.* **2019**, *6* (8), 473-478. DOI: 10.1021/acs.estlett.9b00294.

(7) Yusuf, R. O.; Noor, Z. Z.; Abba, A. H.; Hassan, M. A. A.; Din, M. F. M. Methane emission by sectors: A comprehensive review of emission sources and mitigation methods. *Renew. Sustain. Energy Rev.* **2012**, *16* (7), 5059-5070. DOI: 10.1016/j.rser.2012.04.008.

(8) Hu, G.; Xiao, G.; Guo, Y.; Manning, M.; Chen, L.; Yu, L.; Li, K. G.; May, E. F. Separation of methane and nitrogen using ionic liquidic zeolites by pressure vacuum swing adsorption. *AIChE J.* **2022**, *68*, e17668. DOI: 10.1002/aic.17668©.

(9) Rufford, T. E.; Smart, S.; Watson, G. C. Y.; Graham, B. F.; Boxall, J.; Diniz da Costa, J. C.; May, E. F. The removal of CO_2 and N_2 from natural gas: A review of conventional and emerging process technologies. *J. Pet. Sci. Eng.* **2012**, *94-95*, 123-154. DOI: 10.1016/j.petrol.2012.06.016.

(10) Kim, J.; Maiti, A.; Lin, L. C.; Stolaroff, J. K.; Smit, B.; Aines, R. D. New materials for methane capture from dilute and medium-concentration sources. *Nat. Commun.* **2013**, *4*, 1694-1701. DOI: 10.1038/ncomms2697.

(11) Zhang, J.; Liu, H.; Zhou, F.; Li, X.; Wei, K.; Song, J. Enrichment of oxygen-containing low-concentration coalbed methane with CMS-3KT as the adsorbent. *ACS Omega* **2021**, *6*, 6914-6923. DOI: 10.1021/acsomega.0c06148.

(12) Qian, Z.; Yang, Y.; Li, P.; Wang, J.; Rodrigues, A. E. An improved vacuum pressure swing adsorption process with the simulated moving bed operation mode for CH_4/N_2 separation to produce high-purity methane. *Chem. Eng. J.* **2021**, *419*, 129657-129671. DOI: 10.1016/j.cej.2021.129657.

(13) Bae, J.-S.; Su, S.; Yu, X. X.; Yin, J.; Villella, A.; Jara, M.; Loney, M. Site trials of ventilation air methane enrichment with two-stage vacuum, temperature, and vacuum swing adsorption. *Ind. Eng. Chem. Res.* **2020**, *59* (35), 15732–15741. DOI: 10.1021/acs.iecr.0c02616.

(14) Li, X.; Dutta, A.; Dong, Q.; Rollings-Scattergood, S.; Lee, J. Dissolved methane harvesting using omniphobic membranes for anaerobically treated wastewaters. *Environ. Sci. Technol. Let.* **2019**, *6* (4), 228-234. DOI: 10.1021/acs.estlett.9b00076.

(15) Zhong, D.-l.; Ye, Y.; Yang, C.; Bian, Y.; Ding, K. Experimental Investigation of Methane Separation from Low-Concentration Coal Mine Gas ($CH_4/N_2/O_2$) by Tetra-n-butyl Ammonium Bromide Semiclathrate Hydrate Crystallization. *Ind. Eng. Chem. Res.* **2012**, *51* (45), 14806-14813. DOI: 10.1021/ie300641g.

(16) Yang, X.; Li, Z.; Zhang, C.; Wang, H.; Zhang, E.; Xing, Y.; Xiao, P.; Yang, R. T.; Liu, Y.; Webley, P. A. Practical separation performance evaluation of coal mine methane upgrading with carbon molecular sieves. *Chem. Eng. J.* **2019**, *367*, 295-303. DOI: 10.1016/j.cej.2019.02.134.

(17) Xiao, G.; Xiao, P.; Hoadley, A.; Webley, P. Integrated adsorption and absorption process for postcombustion CO_2 capture. *Front. Chem. Sci. Eng.* **2020**, *15*, 483–492. DOI: 10.1007/s11705-020-1964-3.
(18) Hu, G.; Chen, C.; Lu, H. T.; Wu, Y.; Liu, C.; Tao, L.; Men, Y.; He, G.; Li, K. G. A review of technical advances, barriers and solutions in the power to hydrogen (P2H) roadmap. *Engineering* **2020**, *6* (12), 1364-1380. DOI: 10.1016/j.eng.2020.04.016.
(19) Maruyama, R. T.; Pai, K. N.; Subraveti, S. G.; Rajendran, A. Improving the performance of vacuum swing adsorption based CO_2 capture under reduced recovery requirements. *Int. J. Greenh. Gas Control* **2020**, *93*, 102902. DOI: 10.1016/j.ijggc.2019.102902.
(20) Canevesi, R. L. S.; Borba, C. E.; Silva, E. A. d.; A.Grande, C. Towards a design of a pressure swing adsorption unit for small scale biogas upgrading at. *Energy Procedia* **2019**, *158*, 848-853.
(21) Qie, Z.; Wang, L.; Sun, F.; Xiang, H.; Wang, H.; Gao, J.; Zhao, G.; Fan, X. Tuning porosity of coal-derived activated carbons for CO_2 adsorption. *Front. Chem. Sci. Eng.* **2022**, *16* (9), 1345-1354. DOI: 10.1007/s11705-022-2155-1.
(22) Babu, P. E.; Tejes, P. K. S.; Naik, B. K. Parametric investigation on CO_2 separation from flue gas through temperature swing adsorption process using different sorbent materials. *Carbon Capture Sc. Technol.* **2023**, *7*. DOI: 10.1016/j.ccst.2023.100103.
(23) Guo, Y.; Hu, G.; Chen, K.; Guo, J.; Webley, P. A.; Li, G. K. Capture of dilute methane with a novel dynamic-feed dual-reflux pressure swing adsorption process. *AIChE J.* **2022**, *68*, e17390. DOI: 10.1002/aic.17390.
(24) Saleman, T. L.; Li, G.; Rufford, T. E.; Stanwix, P. L.; Chan, K. I.; Huang, S. H.; May, E. F. Capture of low grade methane from nitrogen gas using dual-reflux pressure swing adsorption. *Chem. Eng. J.* **2015**, *281*, 739-748. DOI: 10.1016/j.cej.2015.07.001.
(25) May, E. F.; Zhang, Y.; Saleman, T. L. H.; Xiao, G.; Li, G.; Young, B. R. Demonstration and optimisation of the four dual-reflux pressure swing adsorption configurations. *Sep. Purif. Technol.* **2017**, *177*, 161-175. DOI: 10.1016/j.seppur.2016.12.007.
(26) Guo, Y.; Jusko, V.; Xiao, G.; Hanekom, J.; Hu, G.; Webley, P. A.; May, E. F.; Li, G. K. Separation of $He/N_2/CH_4$ ternary mixtures by a triple-reflux pressure swing adsorption process. *AIChE J.* **2022**, *68*, e17569. DOI: 10.1002/aic.17569.
(27) Qu, D.; Yang, Y.; Qian, Z.; Li, P.; Yu, J.; Ribeiro, A. M.; Rodrigues, A. E. Enrichment of low-grade methane gas from nitrogen mixture by VPSA with CO_2 displacement process: Modeling and experiment. *Chem. Eng. J.* **2020**, *380*, 122509-122523. DOI: 10.1016/j.cej.2019.122509.
(28) Yang, Y.; Wu, Y.; Liu, H.; Ribeiro, A. M.; Li, P.; Yu, J.; Rodrigues, A. E. Enrichment of ventilation air methane by adsorption with displacement chromatography technology: Experiment and numerical simulation. *Chem. Eng. Sci.* **2016**, *149*, 215-228. DOI: 10.1016/j.ces.2016.04.030.
(29) Qian, Z.; Zhou, Y.; Yang, Y.; Li, P. Methane recovery from low-grade unconventional natural gas by the integrated mode of the conventional/improved vacuum pressure swing adsorption processes. *Fuel* **2023**, *331*, 125717. DOI: 10.1016/j.fuel.2022.125717.
(30) Hu, G.; Zhao, Q.; Tao, L.; Xiao, P.; Webley, P. A.; Li, K. G. Enrichment of low grade CH_4 from N_2/CH_4 mixtures using vacuum swing adsorption with activated carbon. *Chem. Eng. Sci.* **2021**, *229*, 116152. DOI: 10.1016/j.ces.2020.116152.
(31) Liu, Y.; Xiao, S.; Bai, P.; Hu, H.; Jin, L. Adsorption separation performance of H_2/CH_4 on ETS-4 by concentration pulse chromatography. *J. Energy Chem.* **2014**, *23* (2), 213-220. DOI: 10.1016/s2095-4956(14)60138-8.
(32) Majumdar, B.; Bhadra, S. J.; Marathe, R. P.; Farooq, S. Adsorption and diffusion of methane and nitrogen in barium exchanged ETS-4. *Ind. Eng. Chem. Res.* **2011**, *50*, 3021-3034. DOI: 10.1021/ie1014124.
(33) Weh, R.; Xiao, G.; Islam, M. A.; May, E. F. Nitrogen rejection by dual reflux pressure swing adsorption using Engelhard Titanosilicate Type 4. *Ind. Eng. Chem. Res.* **2021**, *59*, 22573−22581. DOI: 10.1021/acs.iecr.0c03768.

(34) Canevesi, R. L. S.; Andreassen, K. A.; da Silva, E. A.; Borba, C. E.; Grande, C. A. Pressure swing adsorption for biogas upgrading with carbon molecular sieve. *Ind. Eng. Chem. Res.* **2018**. DOI: 10.1021/acs.iecr.8b00996.
(35) Wang, Y.; Yang, R. T. Chemical liquid deposition modified 4A zeolite as a size-selective adsorbent for methane upgrading, CO_2 capture and air separation. *ACS Sustain. Chem. Eng* **2019**, *7* (3), 3301-3308. DOI: 10.1021/acssuschemeng.8b05339.
(36) Li, G.; May, E. F.; Webley, P. A.; Huang, S. H.-w.; Chan, K. I. Method for gas separation, US 10562005B2. US 2017.
(37) Weh, R.; Xiao, G.; Islam, M. A.; May, E. F. Nitrogen rejection from natural gas by dual reflux-pressure swing adsorption using activated carbon and ionic liquidic zeolite. *Sep. Purif. Technol.* **2020**, *235*, 116215. DOI: 10.1016/j.seppur.2019.116215.
(38) Weh, R.; Xiao, G.; Ashraful Islam, M.; May, E. F. Upgrading sub-quality natural gas by dual reflux-pressure swing adsorption using activated carbon and ionic liquidic zeolite. *Chem. Eng. J.* **2019**, 123753-123762. DOI: 10.1016/j.cej.2019.123753.
(39) Saleman, T. L. H. Adsorption-based separations of gaseous nitrogen and methane mixtures. The University of Western Australia, 2016.
(40) Kikkinides, E. S.; Yang, R.; Cho, S. Concentration and recovery of carbon dioxide from flue gas by pressure swing adsorption. *Ind. Eng. Chem. Res.* **1993**, *32* (11), 2714-2720. DOI: 10.1021/ie00023a038.
(41) Reynolds, S. P.; Ebner, A. D.; Ritter, J. A. New pressure swing adsorption cycles for carbon dioxide sequestration. *Adsorption* **2005**, *11* (1), 531-536.
(42) Reynolds, S. P.; Mehrotra, A.; Ebner, A. D.; Ritter, J. A. Heavy reflux PSA cycles for CO_2 recovery from flue gas: Part I. Performance evaluation. *Adsorption* **2008**, *14* (2), 399-413. DOI: 10.1007/s10450-005-5980-x.
(43) Reynolds, S. P.; Ebner, A. D.; Ritter, J. A. Stripping PSA cycles for CO_2 recovery from flue gas at high temperature using a hydrotalcite-like adsorbent. *Ind. Eng. Chem. Res.* **2006**, *45* (12), 4278-4294. DOI: 10.1021/ie051232f.
(44) Hu, G.; Zhao, Q.; Manning, M.; Chen, L.; Yu, L.; May, E. F.; Li, K. G. Pilot scale assessment of methane capture from low concentration sources to town gas specification by pressure vacuum swing adsorption (PVSA). *Chem. Eng. J.* **2022**, *427*, 130810. DOI: 10.1016/j.cej.2021.130810.
(45) *Gas Capture Technologies (GCT) Pty., Ltd.* 2023. https://www.gascapture.com.au/ (accessed 2023 1/3).
(46) Águeda Maté, V. I.; Delgado Dobladez, J. A.; Álvarez-Torrellas, S.; Larriba, M.; Martínez Rodríguez, Á. Modeling and simulation of the efficient separation of methane/nitrogen mixtures with $[Ni_3(HCOO)_6]$ MOF by PSA. *Chem. Eng. J.* **2019**, *361*, 1007-1019. DOI: 10.1016/j.cej.2018.12.154.
(47) Erden, L.; Ebner, A. D.; Ritter, J. A. Separation of landfill gas CH_4 from N_2 using pressure vacuum swing adsorption cycles with heavy reflux. *Energ & Fuels* **2018**, *32*, 3488-3499. DOI: 10.1021/acs.energyfuels.7b03534.
(48) Bhatt, T. S.; Storti, G.; Rota, R. Optimal design of dual-reflux pressure swing adsorption units via equilibrium theory. *Chem. Eng. Sci.* **2013**, *102*, 42-56. DOI: 10.1016/j.ces.2013.07.040.
(49) Shang, H.; Bai, H.; Li, X.; Li, J.; Yang, J. Site trials of methane capture from low-concentration coalbed methane drainage wells using a mobile skid-mounted vacuum pressure swing adsorption system. *Sep. Purif. Technol.* **2022**, *295*, 121271. DOI: 10.1016/j.seppur.2022.121271.
(50) General Administration of Quality Supervision, Inspection and Quarantine of the People's Republic of China, Standardization Administration of the People's Republic of China. *Classification and essential property of city gas*; 2018.
(51) Zhou, F.; Xia, T.; Wang, X.; Zhang, Y.; Sun, Y.; Liu, J. Recent developments in coal mine methane extraction and utilization in China: A review. *J. Nat. Gas. Sci. Eng.* **2016**, *31*, 437-458. DOI: 10.1016/j.jngse.2016.03.027.

(52) Sarhosis, V.; Jaya, A. A.; Thomas, H. R. Economic modelling for coal bed methane production and electricity generation from deep virgin coal seams. *Energy* **2016**, *107*, 580-594. DOI: 10.1016/j.energy.2016.04.056.
(53) Na, B.-K.; Koo, K.-K.; Eum, H.-M.; Lee, H.; Song, H. K. CO_2 recovery from flue gas by PSA process using activated carbon. *Korean J. Chem. Eng.* **2001**, *18* (2), 220-227. DOI: 10.1007/BF02698463.
(54) Na, B.-K.; Lee, H.; Koo, K.-K.; Song, H. K. Effect of rinse and recycle methods on the pressure swing adsorption process to recover CO_2 from power plant flue gas using activated carbon. *Ind. Eng. Chem. Res.* **2002**, *41* (22), 5498-5503. DOI: 10.1021/ie0109509.
(55) Chue, K. T.; Kim, J. N.; Yoo, Y. J.; Cho, S. H. Comparison of activated carbon and zeolite 13X for CO_2 recovery from flue gas by pressure swing adsorption. *Ind. Eng. Chem. Res.* **1995**, *34*, 591-598. DOI: 10.1021/ie00041a020.
(56) Liu, C.; Zhou, Y.; Sun, Y.; Su, W.; Zhou, L. Enrichment of coal-bed methane by PSA complemented with CO_2 displacement. *AIChE J.* **2011**, *57* (3), 645-654. DOI: 10.1002/aic.12305.
(57) Lu, B.; Shen, Y.; Tang, Z.; Zhang, D.; Chen, G. Vacuum pressure swing adsorption process for coalbed methane enrichment. *Chin. J. Chem. Eng.* **2021**, *32*, 264-280. DOI: 10.1016/j.cjche.2020.08.043.
(58) Yang, J.; Bai, H.; Shang, H.; Wang, J.; Li, J.; Deng, S. Experimental and simulation study on efficient CH_4/N_2 separation by pressure swing adsorption on silicalite-1 pellets. *Chem. Eng. J.* **2020**, *388*, 124222-124231. DOI: 10.1016/j.cej.2020.124222.
(59) Liu, J.; Shang, H.; Yang, J.; Wang, J.; Li, J.; Deng, S. Novel zeolite/carbon monolith adsorbents for efficient CH_4/N_2 separation. *Chem. Eng. J.* **2021**, *426*, 130163. DOI: 10.1016/j.cej.2021.130163.
(60) Douglas, M.; Ruthven, S.; Farooq, S.; Knaebel, K. *Pressure swing adsorption*; Wiley, 1993.